Annex 2

Urchin harvesting and kelp regrowth in northern Norway under ocean acidification and warming

Authors: Phil Wallhead, Wenting Chen, Laura Falkenberg, Magnus Norling, Richard Bellerby, Sam Dupont, Camilla W. Fagerli, Trine Dale, Kasper Hancke, Hartvig Christie

Contents

A2.1 Introduction

Rising carbon dioxide (CO_2) concentrations in the atmosphere are driving important changes in the oceans. More CO_2 is being absorbed by the ocean, causing chemical changes referred to collectively as 'ocean acidification' (Feely et al., 2004; IPCC 2014). Through the greenhouse effect, increasing atmospheric CO_2 is also causing a rise in global air temperature (often termed 'global warming') which in turn leads to warmer oceans. Such changes can affect marine biota and ecosystems, potentially modifying the provision of ecosystem services to human societies such that human welfare is impacted (Doney et al., 2009; Brander et al., 2014; Falkenberg and Tubb, 2017).

Coastal areas at high latitudes such as northern Norway (>65°N) may be particularly vulnerable to ocean acidification. Carbonate concentrations and seawater buffering capacity are naturally lower here due to low temperatures and riverine/freshwater inputs. Coastal acidification can also be locally exacerbated by eutrophication (Cai et al., 2011; Wallace et al., 2014), coastal upwelling (Feely et al., 2008; Haigh et al., 2015), and the 'biological amplification' effect of remineralization in shallow bottom waters (Bates and Mathis, 2009). Northern Norway and the Barents Sea have also been identified as hotspots of ocean warming in observations over the past three decades (Levitus et al., 2009) and century-scale model projections (Biastoch et al., 2011; Bopp et al., 2013; Renaud et al., 2015).

Under contemporary conditions, coastal areas provide a range of ecosystem services to human societies including provisioning, in particular of animals harvested for food (Ferreira et al., 2016). Within northern Norway an emerging fishery is that for the green sea urchin (*Strongylocentrotus droebachiensis*). High demand on the global market combined with a global shortage of supply and sequential expansion of the harvested area, offer the opportunity to develop a potentially profitable industry (Berkes et al., 2006; Chen and Christie, 2016). In some areas, however, urchins may be regarded as a pest that removes valuable kelp forest (notably sugar kelp *Saccharina latissimi*) through overgrazing, and there may be an interest in culling the urchins to allow kelp regrowth. This regrowth can be beneficial as kelp also provides a range of ecosystem services. For example, in Norway kelp has been commercially harvested for more than 50 years (Vea and Ask, 2011). Kelp forests can also provide nursery grounds, feeding areas or migration routes for fish species of economic value (e.g., coastal cod *Gadus morhua*; Norderhaug and Christie, 2009; Seitz et al., 2013) as well as other ecosystem services such as carbon sequestration, water quality regulation, and cultural services such as diving and recreational fishing (Falkenberg and Tubb, 2017).

Ocean acidification and warming are emerging as external factors that can modify fisheries and their management (Anderson et al.,

2011). It is anticipated that, in the future, managers will need to act to avoid the potentially pervasive negative effects of climate change on a range of economic properties of fisheries, including net present value, revenue, economic yield, and total profits (reviewed by Falkenberg and Tubb, 2017). It may be necessary to modify human harvesting activities such that management of natural resources is optimized.

This study explores optimal harvesting strategies for the emerging urchin fishery in northern Norway, and urchin culling requirements to allow the regrowth of kelp forest. The specific questions asked are: What are the potential impacts of ocean acidification and warming on urchin harvest yield and what are the optimal management strategies for urchin harvesting and culling? A simple kelp-urchin dynamical model is used to explore management strategies in which exhaustive harvesting (or culling) is allowed within a specified area but the minimum harvested (or culled) urchin size is restricted. These simulations allow size limits to be identified that maximize harvest yield or ensure an effective cull during present-day (2000–2020) and future periods (2030–2050 under the SRES A1B scenario).

A2.2 Methods

The dynamics of sugar kelp and green sea urchins were modeled in a non-retentive fjord in northern Norway. The approach loosely follows that of Marzloff et al. (2013) (see Appendix Table A2.1 for details). Briefly, the kelp is modeled as a bulk biomass with logistic growth dynamics, a constant recruitment flux from settling sporelings, and grazing losses proportional to urchin biomass (Eqns A1, A3; Larson et al., 1980; Meidel and Scheibling, 1999). The urchin population is age-structured in classes 0–1, 1–2, …, 14–15 years, neglecting the biomass contributions of individuals >15 years (Fagerli et al., 2015). To account for size-dependent grazing/predation/harvesting effects, the mean and standard deviation of test diameter within each age class are modelled dynamically (Eqn A7) and used to simulate individual test diameters and body/gonad masses (Eqns A8–A10). Urchin recruitment to the 0–1 age class varies stochastically between years and is strongly limited by the presence of kelp (Eqns A2, A4; Fagerli et al., 2013, 2015). Survival between age classes follows a constant, size-independent mortality rate and a predation mortality rate that increases with kelp cover and is reduced for larger individuals (large size refuge) (Eqns A2, A5, A6). Net immigration of individuals older than 1 year into the harvested patch is assumed to be zero. Default model parameter values and uncertainties are derived from statistical model fits to field data (Fagerli et al., 2013, 2015) or based on expert opinion and literature values (Appendix Table A2.2).

The model was configured to represent a patch of area 200 m^2 and was first run for 50 years spin-up without harvesting, starting with zero kelp to produce a steady state urchin barren initial condition. It was then run for a further 20 years with annual harvesting to remove all urchins above a given minimum size. To account for uncertainty the spin-up and harvesting runs were performed as 500-member ensembles with parameter values and stochastic recruitment variability varying between ensemble members following the uncertainty model (Appendix Table A2.2). The harvesting runs were used to explore how the expected harvest yield (as gonad biomass) and its uncertainty varied as a function of the minimum harvested size, assumed to be a fixed constant as a simple management strategy.

Optimal harvesting was investigated first for a present-day scenario, then for a near-term scenario of 0.8°C warming and 100 µatm increase in partial pressure of CO_2 (pCO_2). These physical–chemical changes were based on projections for the period 2030–2050 vs. 2000–2020 under a business-as-usual scenario (SRES A1B) using the SINMOD ocean biogeochemical model (Slagstad et al., 2015). Temperature and pCO_2 sensitivities were parameterized in the kelp growth rate, urchin recruitment flux, and urchin mortality (Appendix Tables A2.1 and A2.2). It is assumed that observed differences in urchin recruitment and mortality between Hammerfest (70.66°N) and Vega (65.67°N) urchin barren sites are associated with bi-decadal mean temperature, with the Vega sites 1.76°C warmer (from bias-corrected SINMOD output, Wallhead et al., 2017). pCO_2 sensitivities were based on literature results from laboratory experiments (see Appendix Table A2.2). Sensitivity of adult urchin growth and mortality to the 100 µatm pCO_2 increase (~0.1 unit decrease in pH) was neglected based on field observations (Uthicke et al., 2016) and experimental results (Siikavuopio et al., 2007; Stumpp et al., 2012; Dupont et al., 2013), noting that the need to interpolate between control conditions and experimental treatments that are much more extreme than +100 µatm pCO_2 introduces some uncertainty. Sensitivity of urchin larval growth rate to the projected acidification was similarly neglected (Chan et al., 2015). Temperature sensitivity of urchin gonad index (ratio of gonad mass to body mass) was based on results from 8-week experiments (Siikavuopio et al., 2006), averaging fractional changes during summer (July–August) and winter (December–January) (Eqn A10), and again using bias-corrected SINMOD output to project seasonal warming (from 8.0°C to 8.8°C for summer and from 6.4°C to 7.2°C for winter).

A2.3 Results and discussion

Model behavior and comparison with observations

The model reproduces the paradigmatic behavior of alternative stable states (May, 1977; Scheffer et al., 2001) with abrupt transitions or 'regime shifts' occurring between kelp forest and urchin barren states (Filbee-Dexter and Scheibling, 2014; Ling et al., 2015). When the urchin recruitment flux, which is probably the most naturally variable parameter, is varied over plausible ranges of interannual variations, the system displays strong hysteresis (Figure A2.1). Starting in an urchin barren state, reducing the recruitment flux reduces the total urchin density (blue line) but does not allow recovery of the kelp forest until a low threshold density is reached, after which a regime shift to a kelp-dominated state occurs (the modelled threshold is perhaps too low compared to the 5–10 individuals per m^2 cited by Leinaas and Christie, 1996). Once in the kelp-dominated state, the recruitment flux must be raised to a high level in order to trigger the reverse shift back to the urchin barren state (red line). This behavior occurs even in the absence of an explicitly-resolved third party such as a higher predator (Marzloff et al., 2013) or recruitment facilitator (Baskett and Salomon, 2010).

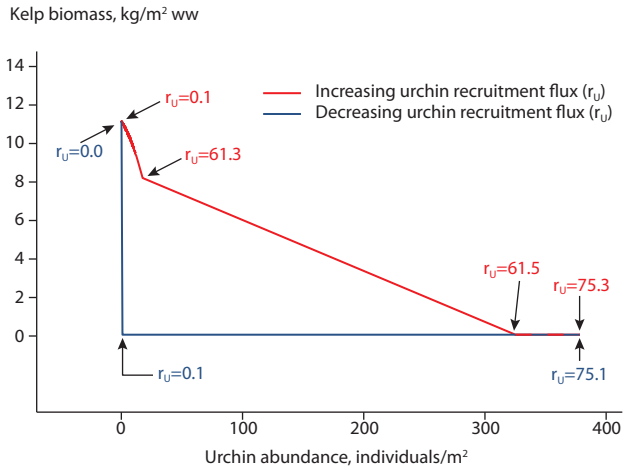

Figure A2.1 Hysteresis plot for the kelp-urchin dynamical model with no stochasticity, varying the parameter r_U (urchin recruitment flux) from 0 to 75.3 and back again to 0.

Comparing with observations from Ling et al. (2015), the model produces a roughly consistent distribution of total abundance density in urchin barrens in northern Norway (Figure A2.2a), allowing for a probable bias in the observations due to undercounting of juveniles (Himmelman, 1986; Russell et al., 1998). This plot provides some independent 'validation', while the remaining comparisons confirm agreement with fitted data. Figure A2.2b shows the exponential decay of abundance over age due to mortality, while Figure A2.2c shows the 'top-heavy' nature of the urchin demographics, with much of the population biomass in the older and less abundant age classes.

Finally, Figure A2.3 shows how the mean size-at-age increases with age, initially at an increasing rate (non von Bertalannfy dynamics). Relative to the Hammerfest barren trajectory, growth is somewhat faster with partial kelp cover (Hammerfest kelp sites). This could not be explained by size-dependent predation alone within the model (not shown), and probably also reflects improved nutrition. Growth in the warmer water (Vega barren) was slightly slower but the same maximum urchin size of around 62 mm is approached in all cases. The effects of kelp presence and warmer water are accounted for in the dynamical model by interpolating between different sets of fitted growth parameters, while the expected shrinking effect of size-dependent harvesting is accounted for by individual-based simulation (see Appendix Table A2.1).

Urchin harvest simulations

In the present-day simulations, the expected annual harvest yield averaged over the 20-year period increases with minimum harvested size until a maximum at around 50 mm is reached, after which it declines (Figure A2.4). Averaging over the first 10 years only, the expected yield is slightly increased and the optimal minimum size is slightly reduced, while the opposite is true if averaging over the last 10 years only. This reflects a decadal population decline and the benefit of looser harvesting restrictions for short-term gains as opposed to the optimal restrictions for 'sustainable' yield. Uncertainty in yield due to parameter uncertainty and stochastic variability is substantial (see error bars). However, this uncertainty has little bearing on the optimal harvesting restriction: to maximize the lower 5%

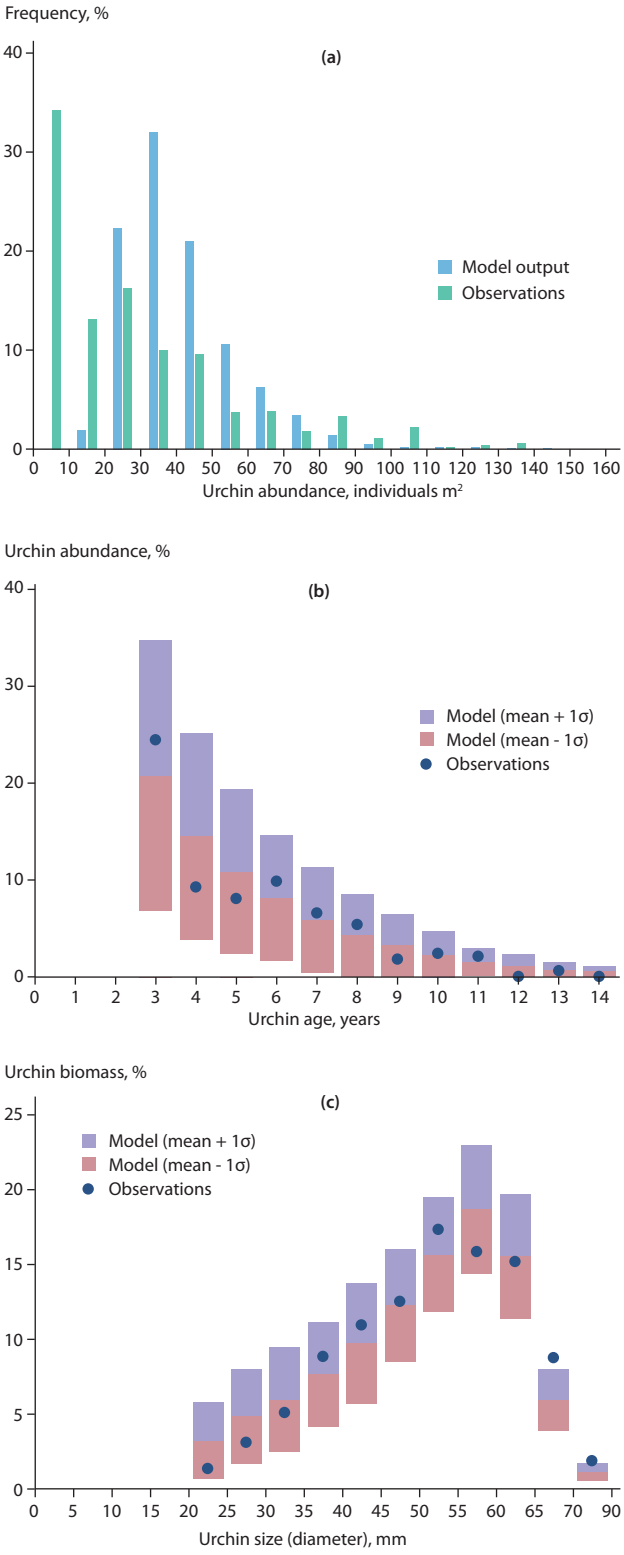

Figure A2.2 The kelp-urchin dynamical model is run 500 times with the default parameter set and stochastic urchin recruitment. Initial conditions are those of an urchin barren. Plot 'a' compares model output with observed data from urchin barrens in Norway north of 68°N (Ling et al., 2015). Each bar shows how frequently an observation or simulation ends in a state with a given urchin abundance range (0–10, 10–20, …, 150–160). Plot 'b' compares model age distribution with observed data from Hammerfest urchin barrens (Fagerli et al., 2015). Only urchins of ages 2+ are considered owing to potential biases in the observations. The graphic shows urchin abundance per one-year age class as a percentage of the total number of urchins of age 2+. Plot 'c' compares model biomass against size-class distribution with observed data from Hammerfest urchin barrens (Fagerli et al., 2015). Only urchins over 20 mm in size are considered owing to potential biases in the observations. The plot shows the amount of urchin biomass per size class as a percentage of the total urchin biomass.

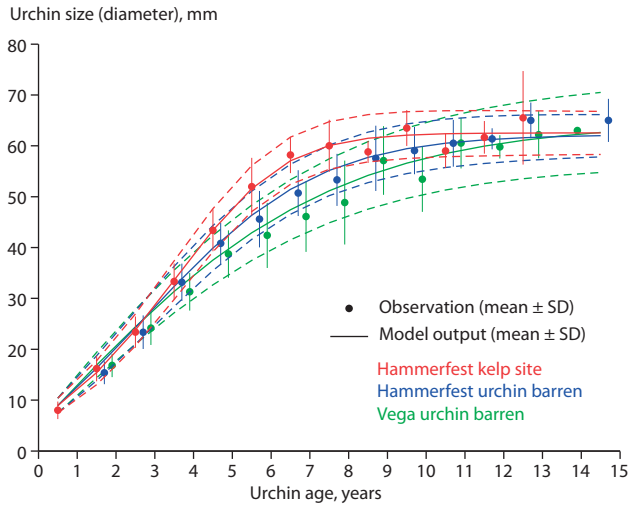

Figure A2.3 Urchin size-at-age relationships in observations from Fagerli et al. (2015) and in the fitted model for the Hammerfest kelp sites, the Hammerfest urchin barren sites, and the Vega urchin barren sites. For clarity, error bars are displaced from age-class central values (0.5, 1.5, …, 14.5 years).

quantile of yield (pessimistic criterion) the optimal minimum size is 45 mm, while to maximize the upper 95% quantile (optimistic criterion) the optimal limit is 50 mm. The optimal limit for any single plausible set of model parameter values and stochastic variability pattern is also well constrained by present knowledge (43–54 mm, 95% CI, not shown). If a limit of 50 mm is applied, the probability of having an urchin barren state, defined as a state with zero kelp, is close to 1 after 20 years.

By contrast, to achieve a high probability (0.8) of provoking a regime shift from an urchin barren to a kelp forest state (defined by kelp biomass ≥0.5 × carrying capacity), it would be necessary to annually cull or remove all urchins ≥10 mm.

In the future simulations, the annual harvest yield is reduced roughly seven-fold due to warming and acidification. However, the optimal harvesting restriction is little affected, remaining close to 45 mm. The culling requirement for a shift to kelp forest with probability 0.8 is slightly relaxed, but remains stringent at around 15 mm.

The apparent robustness of the optimal harvest restrictions may seem surprising, and probably relates to the growth characteristics and mortality rates of the urchins, which are relatively well constrained by data and assumed to be weakly affected by warming and acidification (Figure A2.4; Appendix Tables A2.1 and A2.2). Older urchins are less abundant (because of mortality), but the rate of individual biomass accumulation is maximized at an advanced age because biomass varies roughly as $(\text{size})^3$ and test diameter growth rate only slowly declines with age (Figure A2.3). In addition, gonad index increases with age and body size, further favoring the harvest of larger individuals (gonad mass scales as body mass to the power of 1.47±0.02 in Eqn A10). Harvesting below 50 mm therefore removes many of the most gonad-productive size/age divisions of the population for future years. For comparison, 50 and 51 mm were the minimum legal catch sizes imposed during initial management of the Nova Scotian and Maine green sea urchin fisheries respectively (Miller, 2008; Johnson et al., 2013).

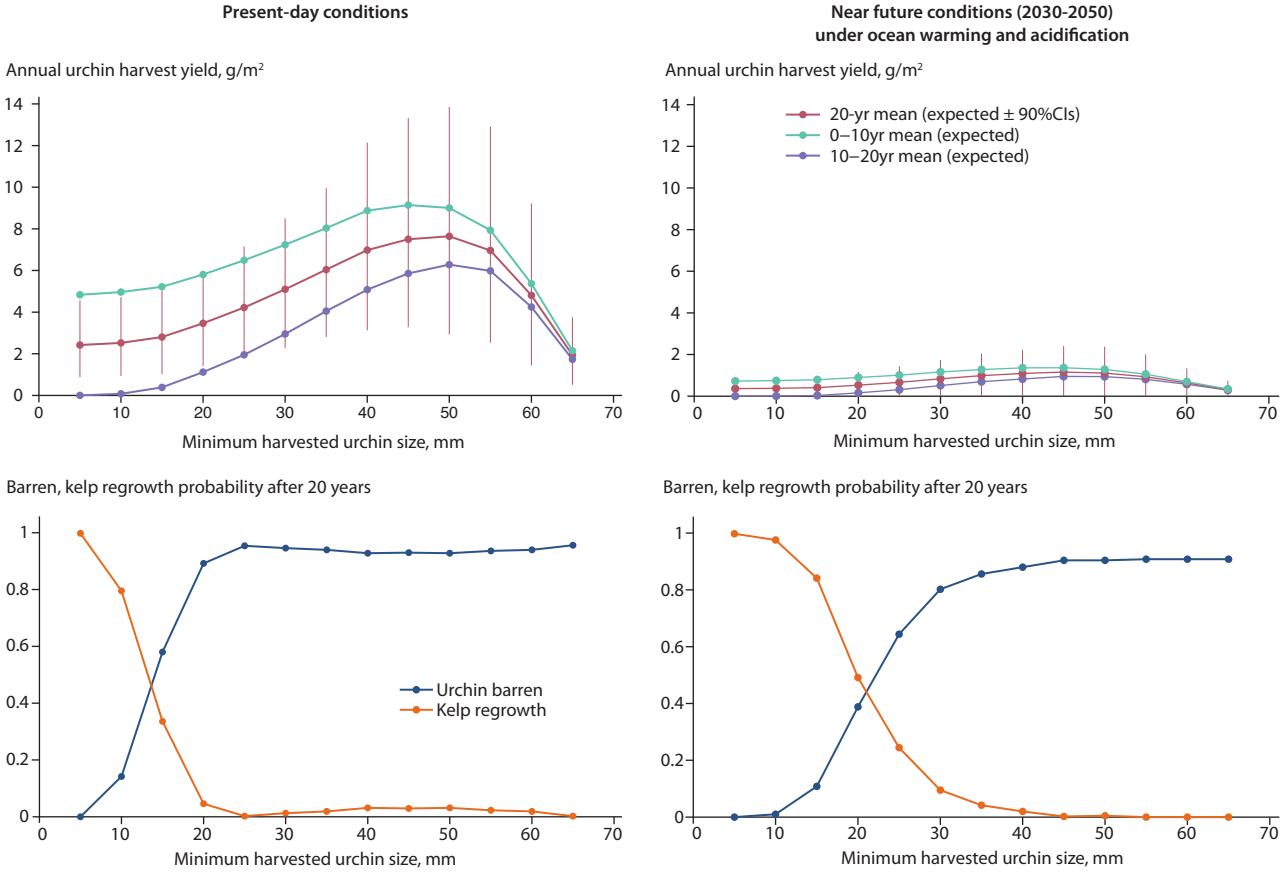

Figure A2.4 Simulated annual urchin harvest yield (gonad biomass per m²) and urchin barren/kelp regrowth probability as a function of the minimum harvested test diameter. Left-hand columns show results for present-day conditions and right-hand columns show the impacts of near-term ocean warming and acidification (2030–2050, SRES A1B, corresponding to +0.8°C, +100 µatm pCO_2 ~ -0.1 pH).

Limitations and recommendations for future work

Population models such as used here (Appendix Table A2.1) have the potential to synthesize information from various sources and propagate individual-scale sensitivities to population-level and economic responses. These models cannot, however, fill basic knowledge gaps regarding individual organism sensitivity. For example, this study assumed log-linear variation to interpolate responses between treatment levels separated by 800 µatm pCO_2 (Appendix Table A2.2). This is clearly open to criticism, and a different interpolating function would yield different responses (e.g., a linear response would give more moderate impacts). Such uncertainties cannot be constrained by purely empirical analysis. More experiments are needed with additional treatments distributed over more moderate levels (regression rather than ANOVA designs). Models of individual-scale physiological response (e.g., DEB models, Jager et al., 2016) are also likely to help in addressing between-replicate variability and other practical limitations of experimental studies.

While ocean acidification had significant impacts on the modelled urchin population through effects on recruitment (10–44% decrease per 100 µatm pCO_2 increase, 95% CI, see $f_{pCO_2}^{r_U}$ in Appendix Table A2.2), the primary factor driving population decline in the future scenario was warming. Based on analysis of field data at Hammerfest (7.0°C) and Vega (8.7°C), warming by just 0.8°C was assumed to decrease recruitment to the 0–1 age class by 44–87% (see $f_T^{r_U}$ in Appendix Table A2.2). As discussed by Fagerli et al. (2013), the observed differences may be partly due to different levels of micropredation on juveniles at the two sites, which may bias the estimate of temperature sensitivity if this effect does not strongly correlate with warming. However, it is not implausible that this is a robust effect on larval survival and embryonic development as summer temperatures approach the 10°C tolerance limit proposed by Stephens (1972) (Rinde et al., 2014). Such precipitous sensitivities of embryonic development have been mapped experimentally for several other echinoderm species (Karelitz et al., 2017: their figure 4) and it seems high time that the response of *S. droebachiensis* be mapped in a similarly quantitative fashion. In general, longer-term and trans-generational sensitivities should be investigated to take into account effects on the different life-history stages, evolutionary processes and trans-generational plasticity (Calosi et al., 2016).

Improved diet through kelp availability may partially compensate the impacts of warming and acidification on urchin recruitment. In the present model this was accounted for using a statistical relationship derived from field data, suggesting a 17–36% increase in gonad index moving from the 'barren' to 'kelp' stations (95% CI, Eqn A10, Appendix Table A2.1). Experiments have shown more dramatic effects of diet on green sea urchins, with gonad indices increased by factors of 2–4 relative to wild populations (Meidel and Scheibling, 1999; Garrido and Barber, 2001; Pearce et al., 2004; Siikavuopio et al., 2006). This suggests a potential for stronger compensation in the future climate, although it seems unlikely that natural improvements will be as extreme as observed in experiments where urchins are fed prepared/optimized food in excess.

It should be noted that this model does not account for effects of kelp regrowth on the local seawater pCO_2 or pH, which may act to compensate the increase in pCO_2 within the harvested patch (Krause-Jensen et al., 2015, 2016). However, results from simulations with 0.8°C warming and no acidification effect (not shown) suggest that even if the pCO_2 increase is fully compensated, there will still be a roughly five-fold decrease in the maximum harvest yield due to warming alone, and the requirements for optimal harvesting and culling will be little affected.

Aside from the warming/acidification responses, the model also assumed no net immigration of urchins older than 1 year into the harvested patch. This will not be valid for small patches or for targeted harvesting patches that cover for example the edges of a kelp forest, where individuals are known to aggregate in grazing fronts (Miller, 2008; Johnson et al., 2012, 2013). In such cases, the influx of immigrants, or 'conveyor belt', may favor more aggressive harvesting strategies and support higher yields per unit area, and indeed may be a prerequisite for a profitable fishing site (Johnson et al., 2013). The present model could be extended to account for net immigration if suitable estimates of immigration rates/fluxes can be obtained. The model also neglected any correlation between annual recruitment to the 0–1 age class and adult abundance within the harvested patch. This is probably a reasonable assumption for non-retentive systems (Fagerli et al., 2013; Marzloff et al., 2013), but would need revision for other systems. However, it seems unlikely that these effects would significantly alter the projected impacts on yield shown in Figure A2.4, as long as the larvae and juveniles that ultimately source the harvested stock are exposed to ocean warming and acidification.

Finally, it should be noted that the default kelp grazing rate of 4% of body mass per day (g_{us} in Appendix Table A2.2) was based on laboratory experiments with urchins fed in aquaria (Larson et al., 1980; Meidel and Scheibling, 1999) and may overestimate the grazing rate in nature, where urchins must move around more in order to graze the kelp. A lower grazing rate is expected to relax the urchin culling requirement for kelp recovery, but additional simulations did not show strong sensitivity of the results (decreasing g_{us} by a factor of 2 over the parameter ensemble raised the culling threshold to ~12 mm and reduced the optimal harvesting limit to 45 mm in present-day simulations, results not shown).

A2.4 Conclusions

This study developed a simple kelp-urchin dynamical model to investigate the potential impacts of ocean warming and acidification on urchin harvest yield and optimal management strategies in northern Norway. Under changes projected for the next 30 years (+0.8°C, +100 µatm pCO_2) urchin harvest yield underwent a roughly seven-fold decrease, while the optimal minimum test diameter (size limit) of harvested individuals remained around 45–50 mm in both present-day and future simulations. In order to provoke a regime shift from an urchin barren to a kelp forest state with high probability, simulations suggested a need to annually cull or remove all urchins larger than 10 mm, and this requirement was also little affected by warming and acidification. These results should be treated as provisional pending further investigation of organism sensitivities at moderate levels of warming and acidification, of grazing rates in natural populations, and of other ecosystem

effects including disease and higher predation. Simplifying assumptions about the harvesting strategy and harvested area, notably that of zero net immigration, may also restrict the validity of present results. On the other hand, the model was able to synthesize information from various sources, including field observations, and was fast to run, enabling an ensemble-based assessment of modeling uncertainty. The model thus appears to be a potentially useful tool for harvest optimization and ecosystem management in the context of a changing climate.

Acknowledgments

Funding is gratefully acknowledged from the NIVA internal SIS (Strategisk instituttsatsning) project 'Coastal Thresholds' and NIVA internal publication funds ('Publispott').

References

Anderson, S.C., J.M. Flemming, R. Watson and H.K. Lotze, 2011. Rapid global expansion of invertebrate fisheries: trends, drivers, and ecosystem effects. PLoS ONE, 6:e14735.

Basket, M.L. and A.K. Salomon, 2010. Recruitment facilitation can drive alternative states on temperate reefs. Ecology, 91:1763-1773.

Bates, N.R. and J.T. Mathis, 2009. The Arctic Ocean marine carbon cycle: evaluation of air-sea CO_2 exchanges, ocean acidification impacts and potential feedbacks. Biogeosciences, 6:2433-2459.

Bates, D., M. Maechler, B. Bolker and S. Walker, 2015. Fitting linear mixed-effects models using lme4. Journal of Statistical Software, 67:1-48.

Berkes, F., T.P. Hughes, R.S. Steneck, J.A. Wilson, D.R. Bellwood, B. Crona, C. Folke, L.H. Gunderson, H.M. Leslie, J. Norberg, M. Nyström, P. Olsson, H. Österblom, M. Scheffer and B. Worm, 2006. Globalization, roving bandits, and marine resources. Science, 311:1557-1558.

Biastoch, A., T. Treude, L.H. Rupke, U. Riebesell, C. Roth, E.B. Burwicz, W. Park, M. Latif, C.W. Boning, G. Madec and K. Wallmann, 2011. Rising Arctic Ocean temperatures cause gas hydrate destabilization and ocean acidification. Geophysical Research Letters, 38: L08602. doi:10.1029/2011GL047222.

Bögner, D., U. Bickmeyer and A. Köhler, 2014. CO_2-induced fertilization impairment in *Strongylocentrotus droebachiensis* collected in the Arctic. Helgoland Marine Research, 01:341-356.

Bopp, L., L. Resplandy, J. C. Orr, S. C. Doney, J. P. Dunne, M. Gehlen, P. Halloran, C. Heinze, T. Ilyina, R. Séférian, J. Tjiputra and M. Vichi, 2013. Multiple stressors of ocean ecosystems in the 21st century: projections with CMIP5 models. Biogeosciences, 10:6225-6245.

Brander, L.M., D. Narita, K. Rehdanz and R.S. Tol, 2014. The economic impacts of ocean acidification. In: Nunes P, Kumar P, Dedeurwaerdere T (Eds.). Handbook on the Economics of Ecosystem Services and Biodiversity. Edward Elgar.

Cai, W-J., X. Hu, W.-J. Huang, M.C. Murrell, J.C. Lehrter, S.E. Lohrenz, W.-C. Chou, W. Zhai, J.T. Hollibaugh, Y. Wang, P. Zhao, X. Guo, K. Gundersen, M. Dai and G.-C. Gong, 2011. Acidification of subsurface coastal waters enhanced by eutrophication. Nature Geoscience, 4:766-770.

Calosi, P., P. De Wit, P. Thor and S. Dupont, 2016. Will life find a way? Evolution of marine species under global change. Evolutionary Applications, 9:1035-1042.

Chan, K.Y.K., E. García and S. Dupont, 2015. Acidification reduced growth rate but not swimming speed of larval sea urchins. Scientific Reports, 5:9764.

Chen, W. and H. Christie, 2016. Sea urchin harvest: ecosystem recovery, integrated management of social-ecological system, ecosystem service and sustainability (ECOURCHIN). Norwegian Institute for Water Research, Norway.

Doney, S.C., V.J. Fabry, R.A. Feely and J.A. Kleypas, 2009. Ocean acidification: the other CO_2 problem. Marine Science, 1:169-192.

Dupont, S., N. Dorey, M. Stumpp, F. Melzner and M. Thorndyke, 2013. Long-term and trans-life-cycle effects of exposure to ocean acidification in the green sea urchin *Strongylocentrotus droebachiensis*. Marine Biology, 160:1835-1843.

Fagerli, C.W., K.M. Norderhaug and H.C. Christie, 2013. Lack of sea urchin settlement may explain kelp forest recovery in overgrazed areas in Norway. Marine Ecology Progress Series, 488:119-132.

Fagerli, C.W., K.M. Norderhaug, H.C. Christie, M.F. Pedersen and S. Fredriksen, 2014. Predators of the destructive sea urchin *Strongylocentrotus droebachiensis* on the Norwegian coast. Marine Ecology Progress Series, 502:207-218.

Fagerli, C.W., S.G. Stadniczeñko, M.F. Pedersen, H. Christie, S. Fredriksen and K.M. Norderhaug, 2015. Population dynamics of *Strongylocentrotus droebachiensis* in kelp forests and barren grounds in Norway. Marine Biology, 162:1215-1226.

Falkenberg, L.J. and A. Tubb, 2017. Economic effects of ocean acidification: publication patterns and directions for future research. Ambio, 46:543-553.

Feely, R.A., C.L. Sabine, K. Lee, W. Berelson, J. Kleypas, V.J. Fabry and F.J. Millero, 2004. Impact of anthropogenic CO_2 on the $CaCO_3$ system in the oceans. Science, 305:362-366.

Feely, R.A., C.L. Sabine, J.M. Hernandez-Ayon, D. Ianson and B. Hales, 2008. Evidence for upwelling of corrosive "acidified" water onto the continental shelf. Science, 320:1490.

Ferreira, B., J. Rice and A. Rosenberg, 2016. The oceans as a source of food. In: The First Global Integrated Marine Assessment (World Ocean Assessment I). United Nations, USA.

Filbee-Dexter, K. and R.E. Scheibling, 2014. Sea urchin barrens as alternative stable states of collapsed kelp ecosystems. Marine Ecology Progress Series, 495:1-25.

Garrido, C.L. and B.J. Barber, 2001. Effects of temperature and food ration on gonad growth and oogenesis of the green sea urchin, *Strongylocentrotus droebachiensis*. Marine Biology, 138:447-456.

Haigh, R., D. Ianson, C.A. Holt, H.E. Neate and A.M. Edwards 2014. Effects of Ocean Acidification on temperate coastal marine ecosystems and fisheries in the Northeast Pacific. PLoS ONE, 10:e0117533. doi:10.1371/journal.pone.0117533.

Himmelman, J.H., 1986. Population biology of green sea urchins on rocky barrens. Marine Ecology Progress Series, 33:295-306.

Iñiguez, C., R. Carmona, M.R. Lorenzo, F.X. Niell, C. Wiencke and F.J. Gordillo, 2016. Increased temperature, rather than elevated CO_2, modulates the carbon assimilation of the Arctic kelps *Saccharina latissima* and *Laminaria solidungula*. Marine Biology, 163:248. doi:10.1007/s00227-016-3024-6.

IPCC, 2014. Climate Change 2014: Synthesis Report. Contribution of Working Groups I, II and III to the Fifth Assessment Report of the Intergovernmental Panel on Climate Change. IPCC, Geneva, Switzerland.

Jager, T., E. Ravagnan and S. Dupont, 2016. Near-future ocean acidification impacts maintenance costs in sea-urchin larvae: identification of stress factors and tipping points using a DEB modelling approach. Journal of Experimental Marine Biology and Ecology, 474:11-17.

Johnson, T.R., J.A. Wilson, C. Cleaver and R.L. Vadas, 2012. Social-ecological scale mismatches and the collapse of the sea urchin fishery in Maine, USA. Ecology and Society, 17:10.5751/ES-04767-170215.

Johnson, T.R., J.A. Wilson, C. Cleaver, G. Morehead and R. Vadas, 2013. Modeling fine scale urchin and kelp dynamics: Implications for management of the Maine sea urchin fishery. Fisheries Research, 141:107-117.

Karelitz, S.E., S. Uthicke, S.A. Foo, M.F. Barker, M. Byrne, D. Pecorino and M.D. Lamare, 2017. Ocean acidification has little effect on developmental thermal windows of echinoderms from Antarctica to the tropics. Global Change Biology, 23:657-672.

Krause-Jensen, D., C.M. Duarte, I.E. Hendriks, L. Meire, M.E. Blicher, N. Marba and M.K. Sejr, 2015. Macroalgae contribute to nested mosaics of pH variability in a subarctic fjord. Biogeosciences, 12:4895-4911.

Krause-Jensen, D., N. Marba, M. Sanz-Martin, I.E. Hendriks, J. Thyrring, J. Cartensen, M.K. Sejr and C.M. Duarte, 2016. Long photoperiods sustain high pH in Arctic kelp forests. Science Advances, 2:e1501938.

Larson, B.R., R.L. Vadas and M. Keser, 1980. Feeding and nutritional ecology of the sea urchin *Strongylocentrotus droebachiensis* in Maine, USA. Marine Biology, 59:49-62.

Leinaas, H.P. and H. Christie, 1996. Effects of removing sea urchins (*Strongylocentrotus droebachiensis*): Stability of the barren state and succession of kelp forest recovery in the East Atlantic. Oecologia, 105:524-536.

Levitus, S., G. Matishov, D. Seidov and I. Smolyar, 2009. Barents Sea multidecadal variability. Geophysical Research Letters, 36: L19604, doi:10.1029/2009GL039847.

Ling, S.D., R.E. Scheibling, A. Rassweiler, C.R. Johnson, N. Shears, S.D. Connell, A.K. Salomon, K.M. Norderhaug, A. Pérez-Matus, J.C. Hernández, S. Clemente, L.K. Blamey, B. Hereu, E. Ballesteros, E. Sala, J. Garrabou, E. Cebrian, M. Zabala, D. Fujita and L.E. Johnson, 2015. Global regime shift dynamics of catastrophic sea urchin overgrazing. Philosophical Transactions of the Royal Society B, 370: 20130269.

Marzloff, M.P., C.R. Johnson, L.R. Little, J.-C. Soulie, S.D. Ling and S.D. Frusher, 2013: Sensitivity analysis and pattern-oriented validation of TRITON, a model with alternative community states: Insights on temperate rocky reefs dynamics. Ecological Modelling, 258:16-32.

May, R.M., 1977. Thresholds and breakpoints in ecosystems with a multiplicity of stable states. Nature, 269:471-477.

Meidel, S.K. and R.E. Scheibling, 1999. Effects of food type and ration on reproductive maturation and growth of the sea urchin *Strongylocentrotus droebachiensis*. Marine Biology, 134:155-166.

Miller, R., 2008. A sea urchin dive fishery managed by exclusive fishing areas. In: Townsend, R.E., R. Shotton and H. Uchida (Eds.), Case studies in Fisheries Self-governance. FAO Fisheries Technical Paper. No. 504, pp. 77-87.

Norderhaug, K.M. and H.C. Christie, 2009. Sea urchin grazing and kelp re-vegetation in the NE Atlantic. Marine Biology Research, 5:515-528.

Olischläger, M., C. Iñiguez, K. Koch, C. Wiencke and F.J.L. Gordillo, 2017. Increased pCO_2 and temperature reveal ecotypic differences in growth and photosynthetic performance of temperate and Arctic populations of *Saccharina latissima*. Planta, 245:119-136.

Pearce, C.M., T.L. Daggett and M.C. Robinson, 2004. Effect of urchin size and diet on gonad yield and quality in the green sea urchin (*Strongylocentrotus droebachiensis*). Aquaculture, 233:237-267.

Renaud, P.E., M.K. Sejr, B.A. Bluhm, B. Sirenko and I.H. Ellingsen, 2015. The future of Arctic benthos: Expansion, invasion, and biodiversity. Progress in Oceanography, 139:244-257.

Rinde, E., H. Christie, C.W. Fagerli, T. Bekkby, H. Gundersen, K.M. Norderhaug and D.Ø. Hjermann, 2014. The influence of physical factors on kelp and sea urchin distribution in previous and still grazed areas in the NE Atlantic. PLoS ONE, 9:e100222. doi:10.1371/journal.pone.0100222.

Russell, M.P., T.A. Ebert, P.S. Petraitis, 1998. Field estimates of growth and mortality of the green sea urchin, *Strongylocentrotus droebachiensis*. Ophelia, 48:137-153.

Scheffer, M., S. Carpenter, J.A. Foley, C. Folke and B. Walker, 2001. Catastrophic shifts in ecosystems. Nature, 413:591-596.

Seitz, R.D., H. Wennhage, U. Bergström, R.N. Lipcius and T. Ysebaert, 2013. Ecological value of coastal habitats for commercially and ecologically important species. ICES Journal of Marine Science, 71:648-665.

Siikavuopio, S.I., J.S. Christiansen and T. Dale, 2006. Effects of temperature and season on gonad growth and feed intake in the green sea urchin (*Strongylocentrotus droebachiensis*). Aquaculture, 255:389-394.

Siikavuopio, S.I., A. Mortensen, T. Dale and A. Foss, 2007. Effects of carbon dioxide exposure on feed intake and gonad

growth in green sea urchin, *Strongylocentrotus droebachiensis*. Aquaculture, 266:97-101.

Sivertsen, K., 2006. Overgrazing of kelp beds along the coast of Norway. Journal of Applied Phycology, 18:599-610.

Slagstad, D., P.F.J. Wassmann and I. Ellingsen, 2015. Physical constrains and productivity in the future Arctic Ocean. Frontiers in Marine Science, 2: doi:10.3389/fmars.2015.00085.

Stephens, R.E., 1972. Studies on the development of the sea urchin *Strongylocentrotus droebachiensis*. I. Ecology and normal development. Biology Bulletin, 142:132-144.

Stumpp, M., K. Trübenbach, D. Brennecke, M. Hu and F. Melzner, 2012. Resource allocation and extracellular acid–base status in the sea urchin *Strongylocentrotus droebachiensis* in response to CO_2 induced seawater acidification. Aquatic Toxicology, 110:194-207.

Uthicke, S., T. Ebert, M. Liddy, C. Johansson, K.E. Fabricius and M. Lamare, 2016. Echinometra sea urchins acclimatised to elevated pCO_2 at volcanic vents outperform those under present-day pCO_2 conditions. Global Change Biology, 22:2451-2461.

Vea, J. and E. Ask, 2011. Creating a sustainable commercial harvest of *Laminaria hyperborea*, in Norway. Journal of Applied Phycology, 23:489-494.

Wallace, R.B., H. Baumann, J.S. Grear, R.C. Aller and C.J. Gobler, 2014. Coastal ocean acidification: The other eutrophication problem. Estuarine, Coastal and Shelf Science, 148:1-13.

Wallhead, P.J., R.G.B. Bellerby, A. Silyakova, D. Slagstad and A. Polukhin, 2017. Bottom water acidification and warming on the western Eurasian Arctic shelves: Dynamical downscaling projections. Journal of Geophysical Research Oceans, 122:8126-8144.

Appendix: Kelp-urchin model formulation and parameterization

Table A2.1 Parameterizations and variables used in the kelp-urchin dynamical model.

Eqn No.	Module	Formulation	Variables [units]
A1	Kelp dynamics	$\frac{dS}{dt}=r_S+\alpha_{Sc}\left(1-\frac{S}{K_S}\right)S-g_{US}UB_G$ $\alpha_{Sc}=(f_T^{\alpha_S})^{\Delta T/1^{\circ}C}(f_{pCO_2}^{\alpha_S})^{\frac{\Delta pCO_2}{100\mu atm}}\alpha_S$ (see note 1)	S = kelp biomass density [kgww/m^2] (see note 1) α_{Sc} = kelp growth rate corrected for (T, pCO$_2$) changes relative to Hammerfest present-day [per year] UB_G = grazing urchin biomass density [kgww/m^2] (see Eqn A3) ΔT = climatic (bi-decadal) change in annual mean temperature [°C] ΔpCO$_2$ = climatic (bi-decadal) change in annual mean pCO2 [µatm]
A2	Urchin dynamics	$U_{i+1,j}=R_{i,(j=1)}+p_{Ui,j-1}U_{i,j-1}$	$U_{i,j}$ = urchin abundance density in year i, age class j [ind/m^2] $R_{i,j}$ = annual recruitment [ind/m^2] $p_{Ui,j}$ = net annual survival probability
A3	Grazing urchin biomass density in year i: UB_{Gi}	$UB_{Gi}=\sum_{k=1}^{n_{sizes}}UBs_{i,k}\gamma_{Gk}$ $UBs_{i,k}=A^{-1}\sum_{inds}UIBM\{s_{k-1}\le UITD<s_k\}$ $\gamma_{Gk}=\frac{1}{\Delta s_k}\int_{s_{k-1}}^{s_k}\omega_G(r)dr$ $\omega_G(s)=\min\left(1,\max\left(0,0.5+\frac{(s-s_{0.5G})}{2ds_{0.5G}}\right)\right)$	$UBs_{i,k}$ = urchin biomass density in year i, size class k [kgww/m^2] A = patch area [m^2] $UIBM$, $UITD$ = urchin individual body mass [kgww] and test diameter [mm] (see Eqns A8, A9) γ_{Gk} = grazing activity factor averaged over size class k $\omega_G(s)$ = grazing activity factor (s_{k-1}, s_k) = (minimum, maximum) urchin size in size class k [mm]
A4	Urchin annual recruitment in year i: R_i	$R_i=f_{Si}^{r_U}f_{Ai}^{r_U}r_{Uc}e^{\varepsilon_{rUi}}$ $f_{Si}^{r_U}=(f_S^{r_U})^{S_i/K_S}$ $f_{Ai}^{r_U}=\max(0,1-\pi\sum_j(0.5\times10^{-3}UTDM_{ij})^2U_{ij})$ $r_{Uc}=(f_T^{r_U})^{\Delta T/1^{\circ}C}(f_{pCO_2}^{r_U})^{\frac{\Delta pCO_2}{100\mu atm}}r_U$ $\varepsilon_{rUi}\sim N(-0.5\sigma_{rU}^2,\sigma_{rU}^2)$	$f_{Si}^{r_U}$= limitation due to kelp cover $f_{Ai}^{r_U}$ = limitation due to substrate area occupied by sea urchins $UTDM_{ij}$ = mean urchin test diameter in year i and age class j [mm] (see Eqn A7) r_{Uc} = annual recruitment corrected for (T, pCO$_2$) changes relative to Hammerfest present-day [ind/m^2] ε_{rUi} = stochastic variation in annual recruitment in year i (lognormal model)
A5	Urchin net annual survival probability in year i, age class j: $p_{Ui,j}$	$p_{Ui,j}=(N_{Ui,j}-N_{UHi,j}^{sim}-N_{UMi,j}^{sim})/N_{Ui,j}$ $N_{UHi,j}^{sim}=\{UITD\ge s_H\}_j$ $N_{UMi,j}^{sim}\sim\{\sum_k^{nsizes}B(N_{Ui,k}^{Hcorr},p_{UMi,k})\}_j$ $N_{Ui,k}^{Hcorr}=\{s_{k-1}\le UITD<\min(s_k,s_H)\}$	$N_{Ui,j}$ = number of urchins in modelled area (year i, age class j) $N_{UHi,j}^{sim}$ = simulated number of urchins harvested (year i, age class j) $N_{UMi,j}^{sim}$ = simulated number of urchin deaths (year i, age class j) $N_{Ui,k}^{Hcorr}$ = number of urchins in year i, size class k after removing harvested individuals $p_{UMi,k}$ = urchin (binomial) mortality probability in year i, size class k
A6	Urchin annual mortality probability in year i, size class k: $p_{UMi,k}$	$p_{UMi,k}=1-p_{Uc}(1-p_{Pi}\gamma_{Pk})$ $p_{Uc}=(f_T^{p_U})^{\Delta T/1^{\circ}C}p_U$ $p_{Pi}=1-(f_S^{p_U})^{S_i/K_S}$ $\gamma_{Pk}=\frac{1}{\Delta s_k}\int_{smin_k}^{smax_k}\omega_P(r)dr$ $\omega_P(s)=\min\left(1,\max\left(0,0.5-\frac{(s-s_{0.5P})}{2ds_{0.5P}}\right)\right)$	p_{Uc} = barren state survival probability corrected for warming p_{Pi} = kelp-associated predation probability (see note 2) γ_{Pk} = kelp-associated predation susceptibility factor averaged over size class k $\omega_p(s)$ = predation susceptibility

A7	(Mean, Standard Deviation) of urchin test diameter in year *i*, age class *j*: ($UTDM_{i,j}$, $UTDSD_{i,j}$)	$UTDM_{i+1,1} = b_0$ $UTDM_{i+1,j>1} = b_{1i} + b_{2i}UTDM_{i,j-1} + b_{3i}(UTDM_{i,j-1})^2 + dUTDM^{sim}_{Hi,j-1}$ $UTDSD_{i+1,1} = c_0$ $UTDSD_{i+1,j>1} = c_{1i} + c_{2i}UTDM_{i,j-1} + dUTDSD^{sim}_{Hi,j-1}$	($dUTDM^{sim}_{Hi,j}$, $dUTDSD^{sim}_{Hi,j}$) = simulated changes in the (means, standard deviations) of urchin test diameters due to harvesting in year *i*, age class *j* [mm] ($b_{1\text{-}3i}$, $c_{1\text{-}2i}$) = parameters of urchin growth dynamics, adjusted for temperature and kelp cover in year *i* (see note 3)
A8	Urchin individual test diameter ($UITD$)	$UITD = UTDM + UTDSD \times \delta_{TD}$ $\delta_{TD} \sim N(0,1)$	δ_{TD} = individual random variation in test diameter within given age class
A9	Urchin individual body mass ($UIBM$)	$\log UIBM = d_0 + d_1 \log UITD + \delta_{BM}$ $\delta_{BM} \sim N(0, \sigma^2_{BM})$ (see note 4)	δ_{BM} = individual random variation in log (body mass) for given test diameter
A10	Urchin individual gonad mass ($UIGM$)	$\log UIGM = e_0 + e_1 \log UIBM + e_2 F_{Diet} + \log f^{GI}_T + \delta_{GM}$ $F_{Diet} = \min(1, \frac{S/KS}{SA_I})$ $f^{GI}_T = 1 + \frac{1}{2}\left(df^{GIs}_T \Delta T_s + df^{GIw}_T \Delta T_w\right)$ $\delta_{GM} \sim N(0, \sigma^2_{GM})$ (see note 4)	F_{Diet} = factor (0–1) accounting for improved diet due to kelp availability f^{GI}_T = adjustment factor for annual urchin gonad index due to warming $df^{GIs/w}_T$ = fractional change in urchin gonad index per 1°C summer/winter warming $\Delta T_{s/w}$ = climatic (bidecadal) change in summer/winter temperature [°C] δ_{GM} = individual random variation in log (gonad mass) for given body mass and diet factor

[(1)]The differential equation for *S* is solved analytically for constant UB_G to give an annual update between the yearly time steps of the age-structured urchin model. For this calculation the grazing biomass UB_G is averaged between values at the start and end of the annual time step.

[(2)]Urchin predation is from various sources (notably crabs and ducks, Sivertsen, 2006) and is assumed to increase with kelp cover (Fagerli et al., 2014); here the net effect is modelled implicitly via increased urchin mortality probability.

[(3)]Parameters (b, c) were fitted to data from Fagerli et al. (2015) (see Figure A2.3). Base values for the dynamical model were taken from the Hammerfest barren fits. These values were adjusted for warming by linearly interpolating between fitted values for Hammerfest and Vega barrens, assuming 1.76°C temperature difference between the two regions. To adjust for kelp cover, the approach taken was to interpolate between fitted values for Hammerfest kelp and barren sites, assuming kelp cover = 0.5 ± 0.1 at the Hammerfest kelp sites. Adjustments were varied to account for uncertainty in the assumed kelp cover at the Hammerfest sites and were capped to avoid extrapolation. Parameter sets (b, c) and their adjustments were varied over the parameter ensemble, accounting for covariances via Cholesky decomposition.

[(4)]Parameters ($d, e, \sigma^2_{BM}, \sigma^2_{GM}$) were fitted to data from Norwegian green sea urchins (Hartvig Christie, NIVA, 03/08/2017 pers. comm.). Fitted equations are: log(UIBM [gww]) = -7.086±0.030 + 2.818±0.008 × log(UITD [mm]), with σ_{BM} = 0.167, and log(UIGM [gww]) = -5.037±0.057 + 1.472±0.020 × log(UIBD [gww]) + 0.266±0.050 × F_{Diet}, with σ_{GM} = 0.980. Parameters (d, e) were varied over the parameter ensemble, accounting for covariances via Cholesky decomposition. Uncertainty in the diet factor due to uncertainty in the assumed level of kelp cover (biomass as a fraction of carrying capacity) at the 'kelp' field station in Indreskjær (SA_I = 0.5 ± 0.1) was accounted for by varying SA_I over the parameter ensemble.

Table A2.2 Parameters used in kelp-urchin dynamical model, showing default values, uncertainty parameters assuming lognormal [LN] or normal [N] distributions, 95% credibility intervals, and basis references/methods. Ensemble parameter values are random sampled from (log)normal distributions with medians defined by the default values and (logarithmic) standard deviations defined by the uncertainty parameters (σ). Sensitivity factors are referenced to present-day climate in a Hammerfest green sea urchin barren.

θ	Meaning [units]	Default value	σ [LN/N]	95% CI	Basis(Note)
r_s	Kelp recruitment [gww/m^2/year]	25	1.0 [LN]	4 – 180	Marzloff et al. (2013)
α_s	Kelp growth rate [year^{-1}]	1.0	0.5 [LN]	0.4 – 2.7	Leinaas and Christie (1996)
$f^{\alpha_s}_{T}$	Sensitivity factor for kelp growth rate per 1°C warming	1.068	0.009 [LN]	1.05 – 1.09	Average of logarithmic gradients from Olischläger et al. (2017) and Iñiguez et al. (2016)
$f^{\alpha_s}_{pCO_2}$	Sensitivity factor for kelp growth rate per 100 µatm pCO_2 increase	1.014	0.017 [LN]	0.98 – 1.05	Average of logarithmic gradients from Olischläger et al. (2017) and Iñiguez et al. (2016)(1)
K_S	Annual kelp carrying capacity [kgww/m^2]	11	0.2 [LN]	7 – 16	Hartvig Christie, NIVA, 17/08/2017 pers. comm.
g_{US}	Urchin grazing rate [gww kelp/gww urchin/year]	14.6	0.2 [LN]	10 – 22	Larson et al. (1980); Meidel and Scheibling (1999)
$s_{0.5G}$	Urchin test diameter for half maximum grazing activity [mm]	20	2 [N]	16 – 24	Camilla W. Fagerli, NIVA, 14/11/2017 pers. comm.
$ds_{0.5G}$	Change in test diameter to reach half maximum grazing activity [mm]	5	0.4 [LN]	2 – 11	Camilla W. Fagerli, NIVA, 14/11/2017 pers. comm.
r_U	Urchin mean annual recruitment into 0–1 year age class [ind/m^2]	12.5	0.25 [LN]	8 – 20	(observed mean abundance in Hammerfest barren) × (expected fraction in 0–1 year age class)(2)
σ_{r_U}	Logarithmic standard deviation in urchin annual recruitment	0.82	0.15 [LN]	0.61 – 1.10	GLMM fit to age-structured data from Fagerli et al. (2015)(3)
$f^{r_U}_{S}$	Sensitivity factor for urchin recruitment at maximum kelp cover	0.025	1.10 [LN]	0.003 – 0.22	GLMM fit to juvenile abundance data from Fagerli et al. (2013)(4)
$f^{r_U}_{T}$	Sensitivity factor for urchin recruitment per 1°C warming	0.20	0.47 [LN]	0.08 – 0.48	GLMM fit to juvenile abundance data from Fagerli et al. (2013)(4)
$f^{r_U}_{pCO_2}$	Sensitivity factor for urchin recruitment per 100 µatm pCO_2 increase	0.71	0.12 [LN]	0.56 – 0.90	Combined sensitivity of egg production, fertilization success, and larval/juvenile survival (Bögner et al., 2014; Dupont et al., 2013) (5)
p_U	Urchin annual survival in reference urchin barren	0.71	0.047 [LN]	0.65 – 0.78	GLMM fit to age-structured data from Fagerli et al. (2015)(3)
$f^{p_U}_{S}$	Sensitivity factor for urchin survival at maximum kelp cover	0.72	0.12 [N]	0.47 – 0.96	GLMM fit to age-structured data from Fagerli et al. (2015)(3)
$f^{p_U}_{T}$	Sensitivity factor for urchin survival per 1°C warming	0.95	0.038 [LN]	0.88 – 1.02	GLMM fit to age-structured data from Fagerli et al. (2015)(3)
$s_{0.5P}$	Urchin test diameter for half maximum predation susceptibility [mm]	50	5 [N]	40 – 60	Camilla W. Fagerli, NIVA, 08/11 pers. comm.
$ds_{0.5P}$	Change in test diameter to reach half maximum predation susceptibility [mm]	5	0.4 [LN]	2 – 11	Camilla W. Fagerli, NIVA, 08/11/2017 pers. comm.
df^{GIs}_{T}	Fractional increase in urchin gonad index per 1°C summertime warming	0.17	0.055 [N]	0.06 – 0.27	Siikavuopio et al. (2006)
df^{GIw}_{T}	Fractional increase in urchin gonad index per 1°C wintertime warming	0.05	0.028 [N]	-0.01 – 0.10	Siikavuopio et al. (2006)

Table notes on following page

(1)Logarithmic gradients were first averaged over temperature treatments within each study; any interaction effects were small compared to the variation in pCO_2 effect between studies.

(2)Based on data from Fagerli et al. (2015), with uncertainty estimated by Monte Carlo simulation, accounting for error in the observed mean abundance and in the model estimates of the expected fraction (dependent on parameter p_U). The resulting correlation in estimates of p_U and r_U is accounted for in the parameter ensemble.

(3)Assuming Poisson sampling errors and lognormal recruitment variability, the observed counts in different age classes should approximately follow a Poisson-lognormal distribution under the dynamical model, with mortality causing a log-linear variation over age (this neglects mortality rate variations due to varying kelp biomass). This is a type of Generalized Linear Mixed-effects Model (GLMM) with Poisson family and log link function. The following function in R was fitted using package 'lme4' (Bates et al., 2015): log(count) ~ Age + Kelp_cover + ΔT+ Age:Kelp_cover + Age:ΔT + (1|Station/Age), where Age is the urchin age in years, Kelp_cover is the kelp biomass as a fraction of carrying capacity (assumed to be 0.5/1.0 in Hammerfest/Vega kelp sites and 0 in urchin barren sites) and ΔT is the difference in bi-decadal average bottom water temperature relative to Hammerfest (=1.76°C for Vega sites, 0°C for Hammerfest sites). This model assumes independent lognormal spatial variability between sampling stations and independent lognormal temporal variability between ages (years) within stations. Counts for ages <2 years were excluded due to likely sampling biases, and counts from Vega kelp forest sites were excluded due to excessive zeros. The fitted coefficients for (Age, Age:Kelp_cover, Age:ΔT) are used to constrain (p_U, f_S^{pU}, f_T^{pU}) in the dynamical model while the other fixed effects are used only to improve model fit since they are probably impacted by variations in sampling effort between stations. The fitted random effect variances were used to place conservative constraints on σr_U, and the covariance matrix of the fixed effects was used to produce covarying ensemble member parameters.

(4)The following Poisson-lognormal GLMM (see note 3) was fitted to the juvenile (<2 cm) urchin abundance per m^2 data from Fagerli et al. (2013): log(count) ~ Kelp_cover + ΔT + (1|sample), hence assuming independent lognormal variability between each abundance sample.

(5)It is assumed that $r_U = Ep_F p_L p_J$ where E is the egg production, p_F is the probability of successful fertilization, and $p_{L,J}$ are conditional probabilities of survival through larval and juvenile stages. Hence the net sensitivity factor is a product of the sensitivities of each process/stage. The 100 µatm sensitivity factors for (E, p_L, p_J) were estimated from Dupont et al. (2013) using only results from acclimated organisms and log-linearly interpolating over the 800 µatm treatment level, hence for example $f^E_{pCO_2} = (E(1200\mu atm)/E(400\mu atm))^{1/8}$. For p_F a log-linear model was fitted to the data up to 1300 µatm from Bögner et al. (2014) and again interpolated back to 100 µatm change. Uncertainties were calculated by Monte Carlo simulation.